Ventricular Fibrillation Dynamics: Manifold Learning and Neural Network Approach

Dafne Lozano-Paredes[1], Juan José Sánchez-Muñoz[2], Luis Bote-Curiel[1], Francisco M Melgarejo-Meseguer[1], Antonio Gil-Izquierdo[3], F Javier Gimeno-Blanes[3], José L Rojo-Álvarez[1]

[1] Department of Signal Theory and Communications. Universidad Rey Juan Carlos, Spain
[2] Arrhythmia and Electrophysiology Unit, Hospital Universitario Virgen de la Arrixaca, Spain
[3] Department of Signal Theory and Communications. Universidad Miguel Hernández, Spain

Abstract

Ventricular Fibrillation (VF) is a critical cardiac arrhythmia characterized by rapid and irregular heartbeats, often leading to sudden cardiac death. Moreover, conventional methods for analyzing the patterns of heart rhythms are not able to fully explore the different origins of VF. Therefore, VF occurring during cardiopulmonary bypass (CPB) surgeries offers a unique opportunity to study how VF develops in real human situations. This research aims to classify the two VF types during CPB (VFON and VFOFF) and understand their mechanisms. The study uses manifold and deep learning techniques to examine VF signals from twelve VFON and seventeen VFOFF patients. Results show successful classification of the frequency evolution of the signal with 81.36% accuracy using Uniform Manifold Approximation and Projection (UMAP) and 90.52% accuracy using Temporal Convolutional Neural Networks. Both methods highlight distinct frequency and pattern variations, with frequency patterns being more easily identifiable than time events.

1. Introduction

Multiple wavelet reentrant electrical activity causes ventricular fibrillation (VF), as shown on an electrocardiogram (ECG), as ultrarapid baseline undulations with uneven timing and morphology. VF causes cardiac arrest, which is characterized by a lack of pulse and unconsciousness. If treatment is not received, sudden cardiac death (SCD) occurs next. VF is initially detected in approximately 10% of cardiac arrest cases [1]. The early treatment of VF may include cardiopulmonary resuscitation (CPR) with a focus on early defibrillation as a means of preventing sudden death. Patients at a high risk of experiencing recurrent VF are treated with implanted cardioverter-defibrillators (ICDs) [1, 2].

Due to the high risk of SCD, understanding the fundamental mechanics of VF can be relevant for discovering the underlying pathology and electrophysiology of the disease. Studies have focused on examining the rate and regularity of VF at various locations and times, with rotors reported to function as fast periodic sources of activation [3]. Determining the dominant frequency of VF using methods such as fast Fourier transform, short-time Fourier transform, and pitch frequency analysis has been suggested [4]. However, the functioning of VF is not entirely clear due to its highly volatile and erratic nature. Some regional variations have been identified, needing further investigation to discover potential sources of VF [3, 4].

In this context, clarifying the various mechanisms underlying VF is essential. Furthermore, studying VF during cardiopulmonary bypass (CPB) can provide valuable insights into its evolution in humans. Therefore, this study employs manifold learning techniques and neural networks to differentiate between the two possible types of VF during CPB: one occurring when the machine starts working, and the other preceding the cessation of machine activity. This approach can offer an understanding of the distinct dynamic properties of VF across different temporal and frequency conditions.

2. Materials and Methods

2.1. The Dataset

In this study, the dataset used has electrocardiogram (ECG) data collected during CPB procedures. Specifically, on the one hand, the dataset includes recordings from twelve patients experiencing the denominating VFON. These episodes are frequent during extracorporeal circulation in cardiac surgery and could represent a natural evolution pattern of VF from its onset to asystole. These episodes were triggered after aortic clamping and perfu-

sion. A CPB was performed with cannulation in the ascending aorta, and systemic temperature was lowered between 28 and 32 °C (moderate hypothermia). Myocardial protection was achieved using cold hyperkalemic blood cardioplegia via antegrade and retrograde routes. On the other hand, seventeen patients experienced episodes of VFOFF that originated from asystole in patients undergoing cardiac surgery with extracorporeal circulation. They were triggered after aortic declamping and restoration of the patient's cardiac circulation. The data was provided by the *Hospital Clínico Universitario Virgen de la Arrixaca (HCUVA)* in Spain. Each recording consists of two ECG leads with a sampling frequency of 200 Hz. A train-test division was performed on the signals of 29 patients to ensure robust evaluation, 18 cases were used to train the model and 11 cases were reserved for testing. The analysis was conducted on both time and frequency windows. For time-based analysis, classification was performed on each time sample. For frequency-based analysis, signals were segmented with overlapping windows, and the Welch periodogram was applied. Ten windows were selected to ensure frequency evolution over time, resulting in an effective window length of 2 seconds.

2.2. Manifold Learning

Supervised Uniform Manifold Approximation and Projection (UMAP) [5] was used for creating low-dimensional representations of high-dimensional data based on algebraic topology and Riemann geometry. This enables the exploration of dynamic characteristics inherent in VF signals over time, considering their spectral characteristics. To do this, UMAP represents the probability of connection between two places using a weighted network. As a result, low-dimensional (3-dimensional) latent spaces show the properties of the VF signals.

There are other methods for dimensionality reduction, such as t-distributed Stochastic Neighbour Embedding (t-SNE) [6]. It operates by giving different points a lower probability and similar points a higher probability. T-SNE initially generates a probability distribution between pairs of high-dimensional objects. Then, t-SNE minimizes the Kullback-Leibler divergence between the two distributions in the low-dimensional map. Therefore, it can reduce high-dimensional data to 3 dimensions, such as network activations inside a layer of the TCN. Thus, the network response in each layer can be visualized.

2.3. Temporal Convolutional Networks

Temporal Convolutional Networks (TCNs) [7] have emerged as powerful tools for analyzing sequential data. Moreover, convolutional neural networks can equal or surpass the performance of recurrent networks, including advantages such as better parallelism, more control over the size of the receptive field, better management of the network memory footprint during training, and more stable gradients.

A dilated causal convolution layer, which functions over each sequence time or frequency step, is the fundamental component of a TCN. Here, the activations calculated at one-time steps do not depend on activations from subsequent time steps. Convolutional layers are usually assembled on top of one another to build context from earlier time steps. Finally, to obtain a larger receptive field, the dilation factor of successive convolution layers is increased exponentially.

3. Experiments and Results

3.1. Manifold Learning with UMAP

UMAP was used to discern differences in frequency evolution between VFON and VFOFF and to visualize the latent space, aiding in understanding data representation and relationships in a lower-dimensional space. As illustrated in Figure 1 (a) and (b), the spatial distribution of VF signals for lead 1 and 2 is represented for both training and testing datasets. , facilitating the examination of its spatial distribution. The application of UMAP enabled the identification of subtle differences in frequency characteristics, effectively distinguishing between VFON and VFOFF.

Embedded spaces from UMAP analysis served as features in a classification model using a linear Support Vector Machine (SVM) to distinguish VFON and VFOFF. The model achieved a final accuracy of 0.8136 and a recall of 0.8910. The confusion matrix in Table 1 (a) depicts classification results based on 2-second window signals capturing frequency evolution.

3.2. Temporal Convolutional Networks

TCNs were utilized to improve classification accuracy for VFON and VFOFF. TCNs operate based on receptive field alterations, with specific parameters employed in the network architecture. In this study, TCNs used 128 filters of size seven across five blocks, with a dropout factor of 0.01 incorporated. They successfully identified frequency evolution differences within VF during surgery phases, achieving an accuracy of 0.9052 and sensitivity of 0.8295.

TCNs are traditionally applied to temporal series data, so we decided to explore their efficacy in identifying patterns of VF signals in time despite the apparent chaotic structure and absence of discernible patterns in these signals. As a result, TCNs demonstrated the ability to detect individual segments within the signals with an accuracy of 0.78 and a sensitivity of 0.7732. Both confusion matrices for the time evolution and frequency evolution used TCNs

		Predicted	
		ON	OFF
Actual	ON	1088	133
	OFF	416	1306

(a)

		Predicted	
		ON	OFF
Actual	ON	93932	27678
	OFF	24010	147602

(b)

		Predicted	
		ON	OFF
Actual	ON	1014	207
	OFF	72	1650

(c)

Table 1. Confusion matrix of the different methods: (a) Confusion matrix of UMAP, where the samples are from the frequency window of 2 seconds; (b) Confusion matrix of TCNs, where the samples are from each sample of the time signal; (c) Confusion matrix of TCNs, where the samples are from the frequency window of 2 seconds.

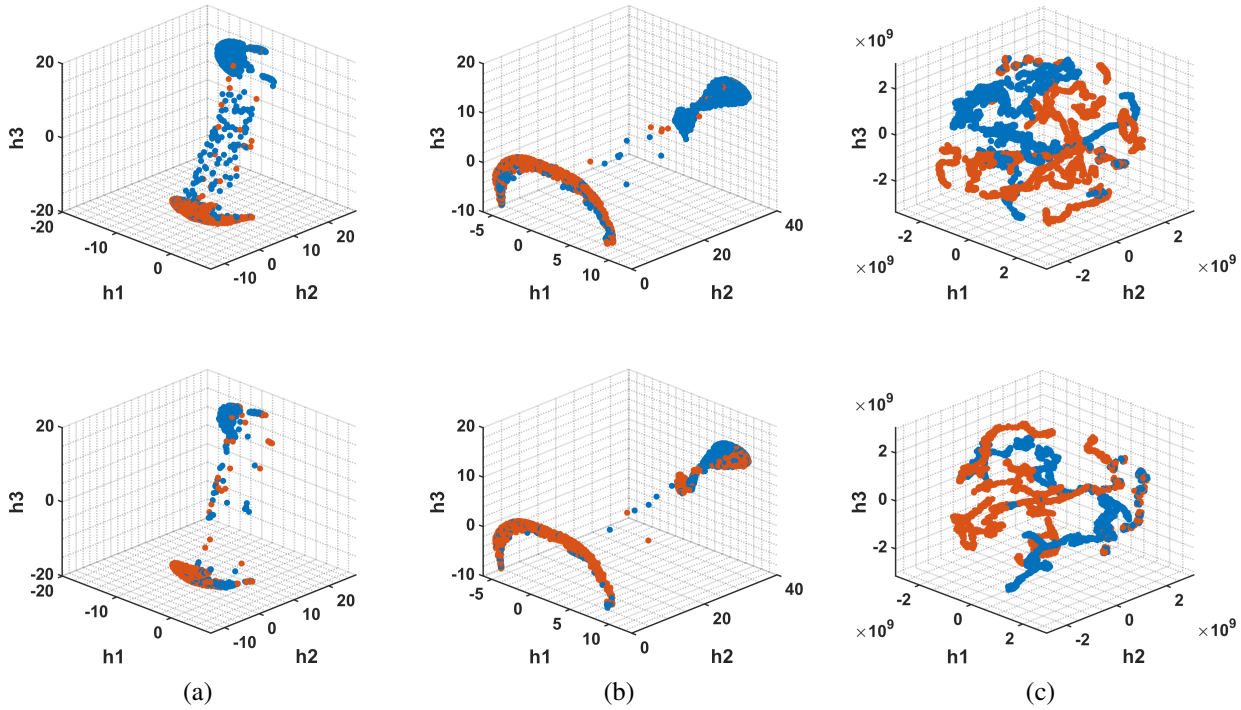

(a) (b) (c)

Figure 1. UMAP and t-SNE embeddings showing VFON and VFOFF classes. Blue denotes represents VFON, and orange represents VFOFF. The train image is positioned at the top while the test is placed at the bottom: (a) UMAP embedding of VF when the signal comes from the first lead; (b) UMAP embedding of VF when the signal comes from the second lead; (c) t-SNE embedding of the two types of VF obtained from the addition layer of the TCN.

can be seen in Table 1 (b) and (c). The classification of each instance can be traced from the frequency window back to the temporal signal, enabling an examination of individual samples within the time domain. Moreover, the relationship is direct for the TCN applied to the time signal, as each sample of the time signal is classified. This can be seen in Figure 2, so we can identify specific misclassified regions. Embeddings can be used to determine how the networks respond in each layer. In this case, we have selected the final addition layer, where the layer adds inputs from multiple previous layers element-wise. The activations in these layers for each type of VF are represented in Figure 1 (c), showing different clusters for VFON and VFOFF types.

4. Discussion

UMAP effectively identified subtle differences in the frequency domain, distinguishing between VFON and VFOFF. It accurately captured the frequency evolution of both VF types, except for short-duration VFON instances and specific segments at the beginning and end of the signals. TCNs demonstrated the ability to detect differential patterns in VF signals over time and frequency. The temporal evolution of the frequency indicates the accurate identification of both types of VF, except for short-

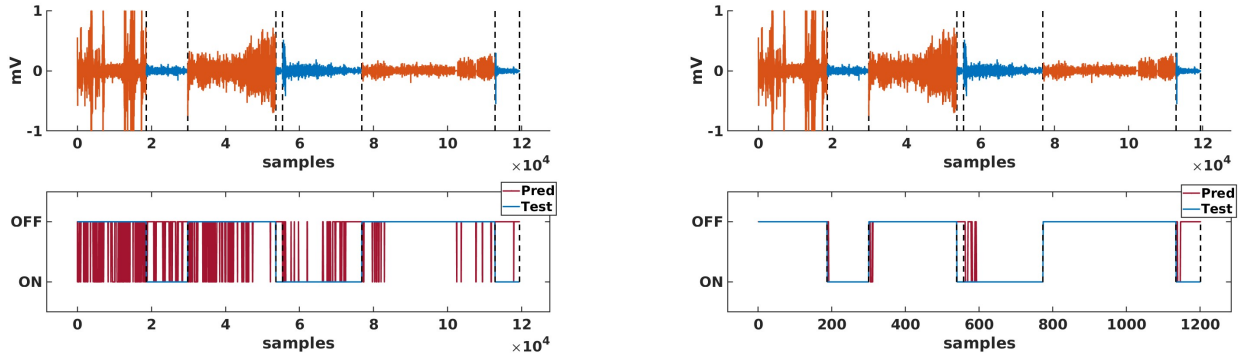

Figure 2. Sample classification after application of TCN to the time signal and frequency evolution of the signal: (a) Time sample classification of 4 signals of FVON (blue) and three signals of FVOFF (orange), each classified instance correspond to a sample in time; (b) Frequency sample (2s windows) classification of 4 signals of FVON (blue) and three signals of FVOFF (orange), each classified instance correspond to a window in time.

duration VFON instances and specific segments at the beginning and end of the signals. On the other hand, for time evolution, the methods struggle to discern patterns in signal regions affected by noise or variations in signal amplitude. Moreover, the latent space visualization of TCN activations revealed how the neural network distinguishes between different VF classes by mapping them to distinct regions, showing clear groupings of VFON and VFOFF instances in training and test datasets.

5. Conclusions

Manifold learning with UMAP and TCNs effectively distinguishes between VFON and VFOFF during CPB, highlighting distinct frequency and temporal patterns. Both methods successfully identify patterns in medium and long-length signals, but they struggle with short-length VFON signals. Future research will improve the detection of subtle differences in shorter VF events.

Acknowledgements

This work was supported by the Research Grants PCardioTrials, LATENTIA, and HERMES (PID2022-140553OA-C42, PID2022-140786NB-C31 and PID2023-152331OA-I00), funded by MICIU/AEI/10.13039/ 501100 011033 and by ERDF/EU, by Research Grant HERMES (Ref.2024/00004/006) from Rey Juan Carlos University, and by a grant to the Madrid ELLIS Unit by Comunidad de Madrid. Thanks to Profs. Jesús Requena-Carrión, Óscar Barquero-Pérez, Paúl Bernal-Oñate, and Vinicio Carrera, for their kind support with data recovery and precedent analysis.

References

[1] Baldzizhar A, Manuylova E, Marchenko R, Kryvalap Y, Carey MG. Ventricular tachycardias: Characteristics and management. Critical Care Nursing Clinics of North America 2016;28(3):317–329. ISSN 0899-5885.

[2] Link MS, Berkow LC, Kudenchuk PJ, Halperin HR, Hess EP, Moitra VK, Neumar RW, O'Neil BJ, Paxton JH, Silvers SM, White RD, Yannopoulos D, Donnino MW. Part 7: Adult advanced cardiovascular life support. Circulation 2015;132(18_suppl_2):S444–S464.

[3] Pandit SV, Jalife J. Rotors and the dynamics of cardiac fibrillation. Circ Res 2013;112(5):849–862.

[4] Latcu GD, Meste O, Duparc A, Mondoly P, Rollin A, Delay M, Maury P. Temporal and spectral analysis of ventricular fibrillation in humans. Journal of Interventional Cardiac Electrophysiology Apr 2011;30(3):199–209.

[5] McInnes L, Healy J, Saul N, Großberger L. UMAP: Uniform manifold approximation and projection. Journal of Open Source Software 2018;3(29):861.

[6] Hinton GE, Roweis S. Stochastic neighbor embedding. In Becker S, Thrun S, Obermayer K (eds.), Advances in Neural Information Processing Systems, volume 15. MIT Press, 2002; .

[7] Bai S, Kolter JZ, Koltun V. An empirical evaluation of generic convolutional and recurrent networks for sequence modeling. CoRR 2018;abs/1803.01271.

Address for correspondence:

Dafne Lozano-Paredes. Dep. of Signal Theory and Communications. University Rey Juan Carlos, Madrid, Spain. Mail to: dafne.lozanop@urjc.es